Drying Characteristics of Distillers Wet Grains Under Varying Condensed Distillers Solubles and Drying Temperature Levels

R. Bhadra, K. A. Rosentrater, K. Muthukumarappan, S. Kannadhason

ABSTRACT. *Distillers dried grains with solubles (DDGS) has been shown to be an excellent livestock feed ingredient, and it is produced by the fuel ethanol industry, which is primarily located in the Midwest United States. There is a growing need to transport DDGS over long distances via rail, but this can often be hampered by poor flowability when unloading. DDGS is formed by combining condensed distillers solubles (CDS) with distillers wet grain (DWG) and then drying at high temperatures. It is hypothesized that drying conditions can affect resulting DDGS chemical, physical, and flow properties, but there is currently little quantified information about drying behavior of these coproducts. Thus, the objective of this study was to investigate the moisture desorption patterns of DWG for three CDS addition levels [10%, 15%, and 20% wet basis (wb)] at three drying temperatures (100°C, 200°C, and 300°C), to thus produce DDGS. Several mathematical models (Page, Newton, Pilosof, Henderson-Pabis, and others) were used to fit the observed moisture data over time. A new comprehensive model was developed for moisture ratio versus time (the best fit had $R^2 = 0.91$, SEM = 0.17) using a modified Page model which accounted for varying CDS and temperature levels. The developed model will be useful to predict moisture content values of DDGS for various drying times, CDS addition levels, and drying temperatures, and will thus be a benefit to industrial processing conditions.*

Keywords. CDS, DDGS, DWG, Desorption, Drying, Moisture content, Moisture ratio, Page model.

The fuel ethanol industry in the United States has experienced rapid growth recently. Researchers and commodity brokers have determined that if fuel ethanol producers were not increasing their output every year, there would have been at least a 15% increase in oil and gasoline prices. That would put oil at more than $115 a barrel, instead of the average price of $102 (Barta, 2008). Distillers dried grain with solubles (DDGS) is one of the main coproducts from the corn-based fuel ethanol industry and is obtained mainly from dry milling production plants. DDGS typically contains 86% to 93% (db) dry matter, 26% to 34% (db) crude protein, 3% to 13% (db) fat, and important amino acids like methionine, leucine, arginine, and threonine (Speihs et al., 2002; Rosentrater and Muthukumarappan, 2006). Due to relatively high protein and energy levels, DDGS is used as livestock feed for both ruminant and non-ruminant animals (Kleinschmit et al.,

2006; Kleinschmit et al., 2007; Mjoun et al., 2007; Mpapho et al., 2007; Bharathan et al., 2008). Besides using DDGS as livestock feed, new uses for DDGS (e.g. as fertilizers, aquaculture feed, and pet litter) have also been reported Cheesbrough et al., 2008; Greenquist et al., 2009; RFA, 2010).

About 16 million metric tons of DDGS were produced in the year 2007-2008 (AAFC Bulletin, 2006); but that rose to nearly 30 million metric tons in 2010 (RFA, 2010). In order to effectively utilize DDGS in domestic and international markets, it is increasingly important to transport DDGS over long distances and to store them (often under varying environmental conditions) for long periods of time. But DDGS often does not easily discharge from hoppers. Poor flowability can significantly affect its utility as a livestock feed. DDGS tends to form "cakes," due to agglomeration of particles, which block or reduce flow. "Caking" (also known as "bridging") is defined as the tendency of DDGS particles to form hard agglomerated masses. Caking and bridging add to the cost of DDGS marketing, since human power, machinery, and time are required to break the agglomerates and unload the affected railcars (Rock and Schwedes, 2005). Agglomerates of DDGS are often broken by using sledge hammers and pick axes, both of which can cause undesirable damage to the rail cars (Bhadra et al., 2009b).

Some possible factors which may be responsible for poor flowability include moisture content, CDS content, fat content, ambient humidity, ambient temperature, particle size, and shape. For example, as CDS level increases, Ganesan et al. (2008c, 2008d) found that DDGS flowability decreases. A significant amount of work has recently been done on various aspects of DDGS flowability, such as: a) inclusion of flow agents to improve flowability (Ganesan

The authors are **Rumela Bhadra, ASABE Member,** Postdoctoral Research Associate, Biological and Agricultural Engineering Department, Kansas State University, Manhattan, Kansas; **Kurt A. Rosentrater, ASABE Member Engineer,** Assistant Professor, Department of Agricultural and Biosystems Engineering, Iowa State University, Ames, Iowa; **Kasiviswanathan Muthukumarappan, ASABE Member Engineer,** Professor, and **Sankaranandh Kannadhason,** Graduate Research Assistant, Agricultural and Biosystems Engineering Department, South Dakota State University, Brookings, South Dakota. **Corresponding author:** Kurt A. Rosentrater, Iowa State University, Department of Agricultural and Biosystems Engineering, 3167 NSRIC Building, Ames, IA 50011; phone: 515-294-4019; e-mail: karosent@iastate.edu.

et al., 2008a), b) measuring physical properties of DDGS and correlating them with Carr (1965) and Jenike (1964) shear test properties (Ganesan et al., 2007a); c) chemical and physical property analysis and development of a flowability model for commercial DDGS samples from local ethanol plants (Bhadra et al., 2009a; Bhadra et al., 2009b), d) development of a predictive flowability model based on exploratory data analysis (Ganesan et al., 2007c), e) determination of dynamic water adsorption (Ganesan et al., 2007b) and sorption isotherm behavior (Ganesan et al., 2008b) of DDGS with varying soluble levels, following Peleg (1988), Pilosof et al. (1985), and Singh and Kulsherestha (1987).

DDGS is produced at dry grind fuel ethanol plants by mixing distillers wet grains (DWG) (containing non-fermentable materials, and is produced by centrifuging water from the whole stillage after fermentation), with condensed distillers solubles (often referred to as CDS or "syrup," which is produced by evaporating the thin stillage from centrifugation). After mixing the wet grains and CDS, the mixed fraction is then subjected to drying, often with drying temperatures of 1000°F (air inlet) and 300°F (air outlet) or more. Drying operations are an integral part of DDGS production, and they affect the final quality and nature of the DDGS produced. They can also affect the flowability of the DDGS. Many technological improvements and changes have been made in the fermentation and distillation steps of ethanol processing over the years, and these changes have increased the efficiency of energy use for ethanol production. However, little attention has been given to issues related to consistency and quality, especially in terms of CDS addition rates and drying conditions. These will affect the resulting physical, chemical, and flowability properties, and ultimately the overall market opportunities for DDGS. Unfortunately, there is no indication of prior research done regarding experimental studies or mathematical modeling of moisture desorption, quantification of drying rate, or moisture diffusion processes for DDGS.

Biological materials, especially grains and foods, have been extensively modeled for drying characteristics. Drying of food and biological materials is an extremely important process, since it has a great effect on end product quality, preservation, and storage (Kingsly and Singh, 2007). Drying kinetics are complex phenomena and require dependable models to predict drying behavior (Sharma et al., 2003). And it is important to have accurate models to simulate drying curves under different drying conditions (Simal et al., 2005). Drying modeling refers to developing abstract mathematical models that can express the relationship between average moisture content and drying time (Pabis et al., 1998). Most research work in this area has focused on thin layer drying, which assumes that the material layer is thin enough or the air velocity is high enough so that the conditions of the drying air (humidity and temperature) are constant throughout the material (Menges and Ertekin, 2006).

Much research has been pursued over the years to develop drying models. For example, researchers have reported mathematical relationships among moisture, drying time, and drying air temperature for pomegranate arils (Kingsly and Singh, 2007), tomato seeds (Sogi et al., 2003), amaranth seeds (Mendoza et al., 2003), apricots (Menges and Ertekin, 2006), wheat grains (Goneli et al., 2007), and mushrooms, pollen, and pistachios (Midilli et al., 2002).

Clearly, there has been much modeling accomplished on the drying behavior of various biological and food materials, but as yet, there has not been a single study regarding drying characteristics or moisture desorption of DWG. Because drying is a key process in the production of DDGS, and drying conditions affect the resulting chemical, physical, and flow properties of DDGS particles, our main objective was to develop comprehensive mathematical desorption models for DWG, and to fit experimental data on these models, which can explain desorption patterns for various CDS addition and drying temperature levels. Mathematical models can provide essential information on the behavior of DDGS under varying operating conditions, and are thus beneficial for facility designers and operators, and can be used to improve handling of DDGS and increase its overall marketability.

MATERIALS AND METHODS

COPRODUCT COLLECTION AND SAMPLE PREPARATION

Samples of distillers wet grains (DWG) and condensed distillers solubles (CDS) were collected from a commercial fuel ethanol plant in South Dakota, and they were stored frozen (-10°C ± 1°C), until experimentation began. For each CDS/DWG combination, CDS was added to DWG at levels of 10%, 15%, and 20% as-is basis [i.e., wet basis (wb)] and then blended thoroughly in a laboratory mixer (AUTOMIX Model no. D300, Hobart Corporation, Troy, Ohio) for 5 min. Each of the CDS/DWG combinations was replicated eight times, yielding 24 (3 × 8) samples, each of which were then subjected to three drying temperatures (thus n=72 total runs in the study), using a full factorial experimental design (table 1). The mixed DWG/CDS samples were placed in plastic bags and stored (-10°C) to prevent microbial spoilage of the samples.

DRYING EXPERIMENTS

Approximately 10 g of each of the CDS/DWG replicates were spread uniformly onto a thin steel plate (which had a diameter of 66.6 mm, height of plate edge of 6.66 mm, plate thickness of 0.60 mm, and a total surface area of 0.0034 m^2). Samples were dried in a laboratory-scale (model no. 838F, Fisher Scientific, Pittsburg, Pa.) oven. Drying was done at one of three temperatures (100°C, 200°C, 300°C) for all samples. These temperatures were based on interviews and discussions with various industry experts (data not

Table 1. Experimental design used for the study.[a]

Treatment	Drying Temperature (°C)	Condensed Distillers Solubles (CDS) (%, wb)
1	100	10
2		15
3		20
4	200	10
5		15
6		20
7	300	10
8		15
9		20

[a] Each treatment was replicated eight times, thus n = 72 total trials in the study.

published). A balance was placed on top of the oven and attached to the sample (using a thin wire cable) to measure changes in sample mass over time (due to drying), as illustrated in figure 1. This dynamic process was used to minimize heat loss and maintain the accuracy of the drying data. For 100°C and 200°C drying temperatures, the experiment was stopped when sample mass values were constant for at least 6 min. For 300°C, however, the mass was recorded every 1 min, due to faster drying rates at this elevated temperature. After all data was collected, moisture loss rates were calculated as dx/dt (change in mass/change in time) in % (db); time was reported in min.

MATHEMATICAL MODELING OF DRYING CURVES

Modeling of drying data was accomplished in two sequential steps. For the moisture content versus time modeling of DWG desorption characteristics, we used moisture content values directly over time and examined the performance of several empirical equations in order to develop an overall global model for moisture content (% db) versus time (min) (table 2) and included terms for CDS and temperature levels. For the moisture ratio versus time modeling, we converted the moisture content (% db) values into a dimensionless quantity, known as moisture ratio, and examined moisture ratio (-) versus time (min) models, which also included terms for CDS and temperature levels. Details of the equations used are given in table 3 and 4. Moisture ratio (MR) is defined as $(X-X_e)/(X_o-X_e)$, where X_e is the equilibrium moisture content (% db), X_o is the initial moisture content (% db), and X is the moisture content (% db) at a particular time. In this stage of modeling, we first used a logarithmic model form, as drying of biological materials is generally a diffusion-controlled process and often may be represented by Fick's law (Sogi et al., 2003). The simplified solution to Fick's law, also known as the logarithmic, or Newton, model is given as:

$$MR = (X-X_e)/(X_o-X_e) = \exp(-kt) \qquad (1)$$

where MR is the moisture ratio (-), X is the moisture content (% db), X_e is the equilibrium moisture content (% db), X_o is the initial moisture content (% db), k is the drying rate constant (time^{-1}), and t is the drying time (min). In this stage of modeling, we also used Page's model, because Page's model has been widely used to describe drying behavior of variety of biological materials and can often yield better results than the logarithmic model (Tan et al., 2001; Sogi
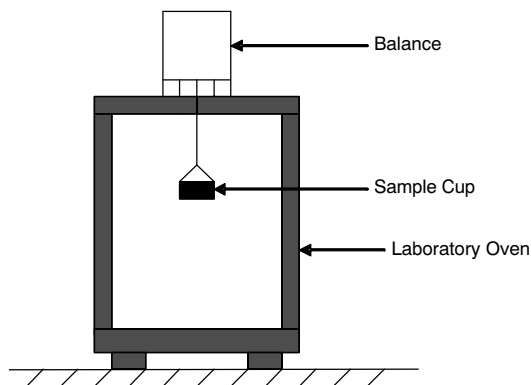
Figure 1. Schematic of experimental set up used to measure sample mass over time.

et al., 2003; Menges and Ertekin, 2006). The Page model is expressed mathematically as:

$$MR = (X-X_e) / (X_o-X_e) = \exp(-kt)^n \qquad (2)$$

where MR is the dimensionless parameter moisture ratio (-), k is the drying rate constant (time^{-1}), t is the time (min), n is the experimental constant to be determined statistically.

We also modified the basic Page model (eq. 2) so that it could encompass the varying CDS and drying temperature levels. Incorporation of CDS and temperature level terms would lead to a unique model that would help predict the desorption behavior of DWG under various operating conditions. Other common models examined for the moisture ratio versus time data for our samples are given in table 3.

The main assumptions for our modeling efforts included:
• constant air flow rate inside the laboratory oven,
• constant humidity during experiments,
• thin layer drying was achieved, and
• the samples achieved thermal equilibrium with the oven.

STATISTICAL ANALYSIS

Parameter estimates for the above models were determined using non-linear regression with the PROC NLIN procedure of SAS v9.1 (SAS, 2002), using the Gauss-Newton method to resolve the models and predict parameter estimates (Seber and Wild, 1989). The standard error of the mean (SEM) between the predicted moisture content (or moisture ratio) and drying rate data is given as:

$$SEM = \sqrt{\frac{\sum (Y_i - \hat{Y}_i)^2}{DF}} \qquad (3)$$

where Y_i and $\hat{Y}_i$ are the experimentally observed and predicted moisture contents (or moisture ratios), respectively, and DF is the degree of freedom (number of data points minus the number of coefficients in the model). PROC NLIN directly provides the F-statistic (F-value) and R^2 (coefficient of determination) values, which are calculated from the model sum of squares, error sum of squares, and total sum of squares. The suitability of each model was determined by comparing the SEM, F-statistic, R^2, and parameter estimate values. An extensive search on previous drying work reveals that these parameters were most often used to determine the validity of the models (Sogi et al., 2003; Doymaz, 2005; Menges and Ertekin, 2006; Ganesan et al., 2007b; Ganesan et al., 2007c; Kingsly and Singh, 2007). Some researchers have also calculated the chi-square test, R^2 - adjusted values, percentage of variance, residual plots, and other various statistical tests to evaluate resulting models (Simal et al., 2005; Menges and Ertekin, 2006; Ganesan et al., 2007c). In this study, a model was considered "good" if it yielded higher R^2 and F-statistic values, relatively smaller SEM values, reasonable parameter estimate values, and most importantly, it yielded a good fit between model-predicted and experimental data.

RESULTS AND DISCUSSION
MOISTURE CONTENT VS. TIME MODELING

Table 2 shows all the models we explored to fit our data using moisture content (% db) as the response variable. As

Table 2. Summary of nonlinear regression output for moisture content vs. time modeling for varying CDS and temperature levels.[a]

No.	Regression Equation	Parameter Estimates					Model Performance					
		A	B	C	D	E	Model SS	Error SS	Total SS	R²	F-statistic	SEM
1	X=Xo*exp(-A*T^C*t)*exp(CDS^D*B)	6.31E-06	0.00109	1.61	1.81		20335506.00	399710.00	20735216.00	0.98	14804.80	58.88
2	X=Xo*exp(-A*T*t)*exp(CDS^B)	0.00039	-1.081				19412273.00	1322944.00	20735217.00	0.94	8554.68	65.50
3	X=Xo*exp(-A*T*t*CDS)	0.000025					18855783.00	1879434.00	20735217.00	0.91	11708.20	68.56
4	X=Xo*(C*CDS)/(A+(B*t*T)	0.467	-7.85E+72	0.03			3414839.00	17320378.00	20735217.00	0.16	230.20	121.89
5	X=(Xo-t/(A+(B*t)))*exp(-D/T)*((CDS*E)+C)	0.0473	0.00476	0.4624	-97.8022	0.00462	18782495.00	1952721.00	20735216.00	0.91	2237.29	230.90
6	X=Xo*exp((-A*T*t)*(B*CDS)/(C*CDS)	0.000432	0.3912	0.03			19418034.00	1317183.00	20735217.00	0.94	8594.64	179.00
7	X=(Xo-t/(A+(B*t)))*exp(-D*T)*((CDS*E)+C)	0.0468	0.00472	1.7317	0.00357	0.0176	18742553.00	1992663.00	20735216.00	0.90	2187.78	236.50
8	X=(Xo-t/(A+(B*t)))*exp(-D/T^2)*((CDS*E)+C)	0.0471	0.00479	0.6104	-6999.8	0.00607	18761433.00	1973784.00	20735217.00	0.90	2210.94	229.50
9	X=(Xo-t/(A+(B*t)))*exp(-D/T^2)*((CDS/E)+C)	0.0471	0.00479	0.6104	-6999.8	164.8	18761433.00	1973784.00	20735217.00	0.90	2210.94	275.36
10	X=(Xo-t/(A+(B*t)))*exp(vD/T^2)*((E/(CDS^2))+C)	0.0469	0.0048	0.202	-7005.9	0.5	18738047.00	1997170.00	20735217.00	0.90	2730.25	173.75
11	X=Xo*(C*CDS)/(A+(B*t^2*T))	4.6703	5.15E+38	0.3			3414839.00	17320378.00	20735217.00	0.16	230.08	122.05
12	X=Xo*(C*CDS)/(A+(B*t*T^2))	4.6703	5.15E+38	0.3			3414839.00	17320378.00	20735217.00	0.16	230.08	122.05
13	X=Xo*exp(-A*T*t)*exp(CDS*B)	0.000403	5.75E-03				19468340.00	1266877.00	20735217.00	0.94	8959.35	65.00
14	X=Xo*exp(-A*T*t)*exp(B/CDS)	0.000386	7.19E-01				19415403.00	1319813.00	20735216.00	0.94	8576.35	265.15
15	X=Xo*exp(-A*T*t)*exp(B/CDS^2)	0.000398	3.15E-04				19471949.00	1263267.00	20735216.00	0.94	8986.34	246.12
16	X=A+B*T+C*CDS+D*exp(-E*t)	115	-0.6591	0.8523	239.8	0.53	4959770.00	1060609.00	6020379.00	0.82	1366.66	30.12
17	X=A+B*t+ C*CDS+D*exp(-T)	4.2139	-0.0534	0.0116	4.583E+43		851.00	1004.70	1855.70	0.46	330.33	178.89
18	X=A+(t*CDS*B) C*exp(-T)	4.2735	-0.00281	4.174E+43			720.90	1134.80	1855.70	0.39	371.98	480.63
19	X=A+B*exp(-C*CDS)+D*t+E*T	288.6	47864456	4808606	-4.0782	-0.6071	3615403.00	2404976.00	6020379.00	0.60	880.18	56.69
20	X=A+B*exp(-C*CDS)+D*t+E*T	288.6	47864456	4808606	-4.0782	-0.6071	3615403.00	2404976.00	6020379.00	0.60	880.18	68.96
21	X=A+ B*exp(-C*CDS)+D*(t+T)	183.1	31060814	3125879	-0.3617		851937.00	5168442.00	6020379.00	0.14	193.19	562.39
23	X=A+ B*exp(-C*(CDS+t))+D*T	152.4	-4.9E+34	5.189E+30	-0.2243		387004.00	5633375.00	6020379.00	0.06	80.51	11968.89
25	X=A+ B*exp-(C*(CDS*T))+D*t	152.1	1	1	-2.4041		1513760.00	4506619.00	6020379.00	0.25	393.67	89.63
26	X=A+ B*exp(-C*(t*T))+D*CDS	91.0209	1.21E+02	1	0.9281		992933.00	5027446.00	6020379.00	0.16	115.64	789.56
27	X=A+ B*exp(-C*(t*CDS))+C*T	134.3	218.1	0.00604	-0.6103		4456696.00	1563683.00	6020379.00	0.74	1111.55	36.56
28	X=A+ B*exp(-C*(t*CDS))+D*T	1	-0.2744599	0.628583	-0.4104109		904.70	951.00	1855.70	0.49	371.00	56.23
29	X=A+ B*exp(-C*(t*T))+D*CDS	4.0521	1.2152	1	0.01		100.60	1755.10	1855.70	0.05	33.57	102.30
30	X=A+1/((B+C)*t +(T+CDS)*D)	-6.3484	-0.9997	1	0.000028		3177034.00	2843345.00	6020379.00	0.53	645.21	75.89
31	lnX=(A-B)- ((C*t)/(D*CDS+E*T))	5.2709	1	8.3694	-692.2	126.6	10.78	1844.92	1855.70	0.01	3.42	4256.89
32	lnX=(A-B)- ((C*CDS)/(D*t+E*T))	5.2597	1	-25.4036	-3339.3	12.3342	32.83	1822.87	1855.70	0.02	10.54	1025.50
33	X=A*CDS/(1+B*exp((-C)*t)^(1/T))	483657	56911.2	-1.6087			14597794.00	6214714.00	20812508.00	0.70	1376.46	1858163.95
34	X=A*CDS/(1+B*exp((-C)*t)^(1/T))	838.8	3064.1	-0.2144			20095.60	3228.20	23323.80	0.86	3647.97	849.82
35	lnX=exp(-A*CDS^B)+C*T+D*t	1843031	-801667	0.0119	0.0406		18985.00	4338.80	23323.80	0.81	2564.15	115.07
36	X=A-((t*CDS*T)/(B*t+ C*CDS))	226.7	5.3083	12.6135			5151605.00	868774.00	6020379.00	0.86	3471.86	31.81
37	X=A-((B*CDS+C*T)*t/D*t)	145.1	-0.00503	0.00117	1		2278823.00	3741556.00	6020379.00	0.38	356.60	25.63
38	X=A-((B*CDS+C*T)*t/D)	201.1	-0.1576	0.0544	1		4920660.00	1099719.00	6020379.00	0.82	2619.80	34.33
39	X=A-(t*CDS/(B*T+ C*CDS))+ D*t	152.1	9.983E+52	-5.89E+30	-2.4041		1513760.00	4506619.00	6020379.00	0.25	393.67	0.51
40	X=A-((t*CDS)/(B*t + C*CDS +D*T))	113.7	145.7	0.886	-80.1157		100729.00	5919650.00	6020379.00	0.02	6.64	2.41
41	X=A-((t*CDS)/(B*t + C*CDS +D*T))	112.09	-1.33E+08	2.44E+08	-8.52E+07		38841.10	5981537.90	6020379.00	0.01	7.61	5.69
42	X=A-((t*CDS)/(B*t + C*CDS +D*T))	111.2	-8.1219	15183.8	-3036.1		70740.20	5949638.80	6020379.00	0.01	6.96	6.51
43	X=A+B*T+C*CDS+D*exp((-E)*t)	115	-0.6591	0.8523	239.8	0.05	4959770.00	1060609.00	6020379.00	0.82	13366.66	30.12
44	X=A-((t*CDS)/(B*t+ C*CDS +D*T))	Did not converge										
45	X=A+ B*exp((-C)*(T+t))+D*CDS	Did not converge										
46	X=A+1/(B*CDS+C*(T+ t))	Did not converge										
47	lnX=A+1/(B*CDS+C*(T+ t)	Did not converge										
48	X=A+1/(B*CDS+C*T+D*t)	Did not converge										
49	X=A+B*CDS+C*T+D/(1-E*exp((-F)*t))	Did not converge										
50	X=A+1/(B*T+C*CDS+D*t)	Did not converge										
51	X=A+1/((B+C)*T +(CDS+t)*D)	Did not converge										
52	X=A+1/((B+C)*CDS +(T+t)*D)	Did not converge										
53	lnX=A+1/((B+C)*CDS +(T+t)*D)	Did not converge										
54	X=A+1/((B+C)*T+(t+CDS)*D)	Did not converge										
55	lnX=A+1/((B+C)*T +(t+CDS)*D)	Did not converge										
56	X=(A-B)-(t/(C*CDS+D*T))	Did not converge										
57	X=(A-B)-((C*t)/(D*CDS+E*T))	Did not converge										
58	X=(A-B)-(CDS/(C*t+D*T))	Did not converge										
59	X=(A-B)-(T/(C*CDS+D*T))	Did not converge										
60	X=(A-B)-(T/(C*CDS+D*T))	Did not converge										
61	lnX=(A-B)-((C*T)/(C*CDS+D*T))	Did not converge										
62	X=A+ B*exp(-C*(CDS+T))+D*t	Did not converge										
63	X=A-((t*CDS)/(B*t+ C*CDS+D*T))	Did not converge										

[a] X is moisture content (% db) at a given time, Xo is initial moisture content (% db), t is time (min), T is temperature (°C), CDS is level of condensed distillers solubles (% wb), A through E are empirical parameter estimates for the model terms, SS is the sum of squares; SEM is the standard error of the mean.

Table 3. Basic mathematical models used to examine moisture ratio vs. time data.[a]

No.	Model Equation	Common Name	Reference
1	MR=exp(-kt)	Newton	Ayensu (1997)
2	MR=exp(-kt^n)	Page	Menges and Ertekin (2006)
3	MR=A*exp(-kt)	Henderson and Pabis	Henderson and Pabis (1961)
4	MR=A*exp(-kt) + c	Logarithmic	Midilli et al. (2002)
5	MR=A*exp(-kt) + (1-A) *exp (-kAt)	Two term exponential	Sharaf-Elden et al. (1980)
6	MR=1+At+Bt^2	Wang and Singh	Ozdemir and Devres (1999)
7	MR=A*exp(-kt^n) + Bt	Midilli et al.	Midilli et al. (2002)
10	MR=Bt/(Bt+1)	Sing-Kulshrestha	Singh and Kulshrestha (1987)
11	MR=A(1-B*exp(-kt))+C	Mechanistic growth	Draper and Smith (1998)
12	MR=A/(1+B*exp(-kt))	Logistic growth	Draper and Smith (1998)
13	MR=A*exp(-B*exp(-kt))	Gompertz model	Draper and Smith (1998)

[a] MR is defined as moisture ratio (-) given as = $(X-X_e)/(X_o-X_e)$; X is moisture content (% db) at a given time; X_o is initial moisture content (% db); X_e is equilibrium moisture content (% db); t is time (min); A, B, C, k, and n are empirical parameter estimates for the model terms.

clearly shown, the standard error of the mean (SEM) values were substantially higher than the SEM values obtained for moisture ratio versus time modeling (table 4). This meant that using moisture ratio actually resulted in a better fit than did moisture content. From table 2 we can also observe that for models 1, 2, and 43 there were relatively high F-values (14804.80, 11708.20, and 13366.66, respectively) but they exhibited very high SEM values (58.88, 68.56, and 30.12, respectively), when compared to models G4 and G17 (table 4). Again from table 2, we can clearly observe that equations 39, 40, 41, and 42 showed lower values of SEM, which indicated better fits for the experimental data, but they also showed much lower F-values, and somewhat odd parameter estimate values; overall they provided poor model fitting

Table 4. Summary of nonlinear regression output for moisture ratio vs. time modeling for varying CDS and temperature levels.[a]

No.	Regression Equation	Equation Name	k	A	B	C	n	Model SS	Error SS	Total SS	R^2	F-statistic	SEM
G1	MR=A*CDS*exp(-k*T*t)	Modified Newton model	0.00	0.06				299.30	36.91	336.21	0.89	4728.36	0.21
G2	MR=A*CDS*exp((-k*t)/T)	Modified Newton model 1	1.61	0.03				235.60	100.70	336.30	0.70	1364.50	0.29
G3	MR=exp(-k*t)/(T*CDS)	Modified Newton model 2	208.60					192.40	143.80	336.20	0.57	1516.12	0.52
G4	MR=exp(-k*T*t*CDS)^n	Modified Page model 1	0.00148				0.02	304.60	31.67	336.27	0.91	11222.10	0.17
G5	MR=exp(-k*t)+(1-A)*exp((-k*CDS*t)/T)	Modified 2 term exp model 1	0.07	16.28				262.40	73.81	336.21	0.78	2072.64	13.60
G6	MR=1+(A*t)+((B*t*CDS)/T)	Modified Wang & Singh 1		-0.05	0.18			232.30	103.90	336.20	0.69	1302.80	0.30
G7	MR=1+(A*t)+((B*t^2)/(CDS*T))	Modified Wang & Singh 2		-0.04	0.63			242.80	93.47	336.27	0.72	1514.28	0.28
G8	MR=1+(A*t*CDS)+((B*t^2)/T)	Modified Wang & Singh 3		0.00	0.04			195.10	141.10	336.20	0.58	806.36	0.34
G9	MR=1+(A*t*T)+((B*t^2)/CDS)	Modified Wang & Singh 4		-0.0003	0.0028			311.60	24.68	336.28	0.93	7359.90	0.15
G10	MR=A*exp(-k*t)+((B*t*CDS)/T)	Modified Henderson & Pabis 1		0.87	0.04	0.08		285.30	50.91	336.21	0.85	2176.42	0.24
G11	MR=A*exp(-k*t)+((B*t*T)/CDS)	Modified Henderson & Pabis 2		0.73	-0.0019	-0.0043		296.80	39.45	336.25	0.88	2921.72	0.19
G12	MR=A*exp(-k*t)+(B*t*T*CDS)	Modified Henderson & Pabis 3		0.72	0.00	-0.0048		295.00	41.27	336.27	0.88	2775.21	0.19
G13	MR=exp(-(k)*t)+A*t/CDS+B*t/T	Modified Henderson & Pabis 4	0.08	-0.12	1.33			291.50	48.20	339.70	0.85	2220.28	0.21
G14	MR=exp((-k)*t^T)+ A*t/CDS	Modified Henderson & Pabis 5	0.21	0.14				137.20	202.50	339.70	0.40	388.30	1.24
G15	MR=exp((-K)*t+ A*t*T/CDS	Modified Henderson & Pabis 6	0.06	0.00				264.40	75.30	339.70	0.82	2648.47	0.24
G16	MR=exp((-K)*t)+A*t/(CDS+T)	Modified Henderson & Pabis 7	0.09	0.54				286.30	53.40	339.70	0.84	3005.78	0.22
G17	MR=exp((-k)*t)+A*t/CDS+B*T*t	Modified Henderson & Pabis 8	-0.01	-0.02	0.00			316.20	23.50	339.70	0.94	5791.11	0.14
G18	MR=exp((-k)*t)+ A*t/CDS +B*T^t	Modified Henderson & Pabis 9				Did not converge							
G19	MR=exp((-k)*t)+ A*t/CDS +B*t/T +C	Modified Henderson & Pabis 10	0.05	-0.13	1.80	-0.22		55.73	43.13	98.86	0.56	504.44	1.24
G20	MR=exp((-k)*t^T)+ A*t/CDS+ B	Modified Henderson & Pabis 11	1.12	-0.14	0.20			6.74	86.87	93.61	0.07	44.39	2.56
G21	MR=exp((-k)*t)+ A*t*T/CDS +B	Modified Henderson & Pabis 12	0.37	-0.45	0.74			34.97	63.90	98.86	0.35	320.67	0.89
G22	MR=exp((-k)*t)+ A*t/(CDS+T)+B	Modified Henderson & Pabis 13	0.06	1.81	-0.99			49.85	289.85	339.70	0.50	595.99	98.86
G23	MR=exp((-k)*t)+ A*t/CDS +B*T^t +C	Modified Henderson & Pabis 14				Did not converge							
G24	MR=exp((-k)*t)+A*t/CDS+B*t/(T+C)	Modified Henderson & Pabis 15	0.07	-0.08	-0.19	-144.60		296.90	42.80	339.70	0.87	2033.01	0.23
G26	MR=exp((-k)*t^T)+ A*t/(B+CDS)	Modified Henderson & Pabis 16	1.21	4.57	409.20			142.00	197.70	339.70	0.42	274.00	6.90
G27	MR=exp((-k)*t)+ A*t*T/(B+CDS)	Modified Henderson & Pabis 17	1.00	0.07	-0.05			316.00	23.70	339.70	0.93	5209.85	14.05
G28	MR=exp((-k)*t)+A*t/(CDS+T+B)	Modified Henderson & Pabis 18	0.09	0.10	-95.22			289.70	50.00	339.70	0.85	2111.57	0.24
G29	MR=exp((-k)*t)+A*t/CDS+(B*T*t)/C	Modified Henderson & Pabis 19	-0.01	-0.02	0.00	1.00		316.20	23.50	339.70	0.94	5791.11	0.29

[a] For base models refer to table 2; MR is moisture ratio (-) given as = $(X-X_e)/(X_o-X_e)$, t is time (min) X is moisture content (% db) at a given time; X_o is initial moisture content (% db); X_e is equilibrium moisture content (% db); T is temperature (°C); CDS is level of condensed distillers solubles (% wb); k, A, B, C, k, and n are empirical parameter estimates for the model terms; SEM is the standard error of the mean; SS is the sum of squares; model G4 (in bold) represents the final selected overall model for MR = f (T, CDS).

results. From table 2, we can also observe that out of 63 possible equations examined, 19 of the equations did not converge, and thus were rejected for model selection purposes.

The initial moisture contents of the samples were approximately 250% (db) for all CDS/temperature level combinations. This was similar to the initial values for thin layer drying experiments by Kingsly and Singh (2007). Most of the methods of parameter estimation (such as least squares, maximum-likelihood, and robust estimation) use an estimate, $\hat{\theta}$, and minimize the function h(θ) iteratively, so that the sequence converges to our estimated value of $\hat{\theta}$. In our case, we used the Gauss-Newton method to approximate h(θ), and minimization was done by a quadratic function, which was due to the fact that the underlying principle used in the Newton method works best for functions which are quadratic (Seber and Wild, 1989). Other methods are also available for non-linear modeling besides the Gauss-Newton method, and convergence criteria can be achieved by changing initialization parameters, maximum likelihood estimation, etc.; we did not try these other methods, however.

One reason that the moisture content versus time models did not work well for the DWG in this study was because the modeling of desorption characteristics is based on the mathematical principles of thin layer drying, which is the most popular form of modeling and simulation of agricultural materials. In thin layer drying models, the rate of change in material moisture content during the falling rate drying period is proportional to the instantaneous difference between material moisture content and the expected material moisture content when it reaches equilibrium with the drying air (Menges and Ertekin, 2006). Thus, moisture ratio, which is the relative moisture content, is actually a better response variable than moisture content, for mathematical modeling of thin layer drying behavior of biological samples.

From table 2, models 1, 16, 36, 38, 39, and 43 showed relatively good R^2, SEM, and F-values, and thus appeared to be potentially viable models; however, the residual plots (fig. 2) strongly suggest that these selected models actually did not result in adequate models. Residuals are calculated from the observed and predicted response variable, and are given as:

$$e_i = Y_i - \hat{Y}_i \qquad (4)$$

where e_i is the calculated residual, Y_i is an observed response value, and $\hat{Y}_i$ is the predicted value based on the model equation used. Thus residuals are the quantitative amount of error that the regression equation was not able to explain (Draper and Smith, 1998). Residual plots are developed by plotting residuals versus predicted response values, and they are used to examine the adequacy of the prediction model.

Model 1 (from table 2) showed high R^2 value (0.98), but from the residual plot (fig. 2) we see it gave an undesired residual plot. First, the residuals were not distributed uniformly and evenly along the x-axis; all the residuals yielded negative values, indicating that the predicted values were all significantly higher than the observed moisture content. Again from table 2, model 16 showed an R^2 value of 0.82 and SEM of 30.12. However, we deemed it inadequate, as the residual plot (fig. 2) did not show random distribution,

some negative values of predicted moisture content were present, and patterns were evident. Models 36 and 38 yielded fairly random and even distributions of residuals over the x-axis, but some negative predicted values of moisture content were observed, as depicted in figure 2. Thus, we also rejected models 36 and 38, even though they had high R^2 values (0.86 and 0.82, respectively). Model 39 showed a low SEM value (0.51), which suggested a good fit, but from figure 2 we can clearly see there was no random distribution of the residuals; patterns in the residual plot are evident. Similar results were obtained for model 43, even though it produced a high F-value (13366.66) and R^2 (0.82); residual plots indicated curved bands of data points, which indicated that a possible higher order term needed to be added to the model equation. Thus, models 1, 16, 36, 38, 39, and 43 were rejected, even though there was evidence of higher R^2, F-value, and lower SEM. All other models for moisture content as a function of time were deemed inadequate as well.

MOISTURE RATIO VS. TIME MODELING

Table 3 indicates the list of various base models that were examined for modeling moisture ratio versus time and were subsequently modified by incorporating CDS and temperature levels terms. Only the logarithmic model (table 3) failed to converge. After examining the performance of all the models provided in table 3, it became evident that only five of them (Newton, Page, exponential, Wang and Singh, and Henderson and Pabis) would yield acceptable results. Of all the models examined, G4 (table 4) appeared to perform the best.

From table 4, we observe that model G17, based on the Henderson and Pabis equation, showed a higher R^2 value (0.94) and lower SEM value (0.14) compared to model G4, but it was not selected as the "best model" because there were some negative predicted values of moisture ratio for t > 20 min at 200°C, which was possibly due to the negative values of "k" (the drying rate constant, time^{-1}) and "A." Again, from table 4, we can also observe that model G29 showed an R^2 value of 0.94 which was higher than our selected model G4. However, model G29 had a lower F-value (5791.11) and higher SEM value (0.29), which indicated that it fit a little less well than model G4. Thus, model G4 was selected as the best equation for modeling moisture ratio vs. time, including CDS and temperature effects.

The predicted MR values obtained using model G4 (which was based on the Page model) exhibited good fit for the MR values, both when it was applied to the temperature and CDS level combinations individually, and when it was globally applied to the entire dataset, as shown in figures 3a and 3b, respectively. Similar results were obtained for the drying of pomegranate arils; out of four different models examined, the Page model worked best (with R^2 of 0.99) for all temperatures (Kingsly and Singh, 2007). However, in that particular study they only modeled the response variable moisture ratio as a function of time (Page's basic model), and did not include temperature and or other parameters. Some work related to drying behavior of tomato seeds also revealed that drying behavior (moisture ratio vs. time) was well described by Page's model (Sogi et al., 2003).

In another study (Simal et al., 2005), the Page model explained nearly 99% of the variance in the drying of kiwi fruits; the diffusion model provided the least exact model, while the Page model provided the best description of
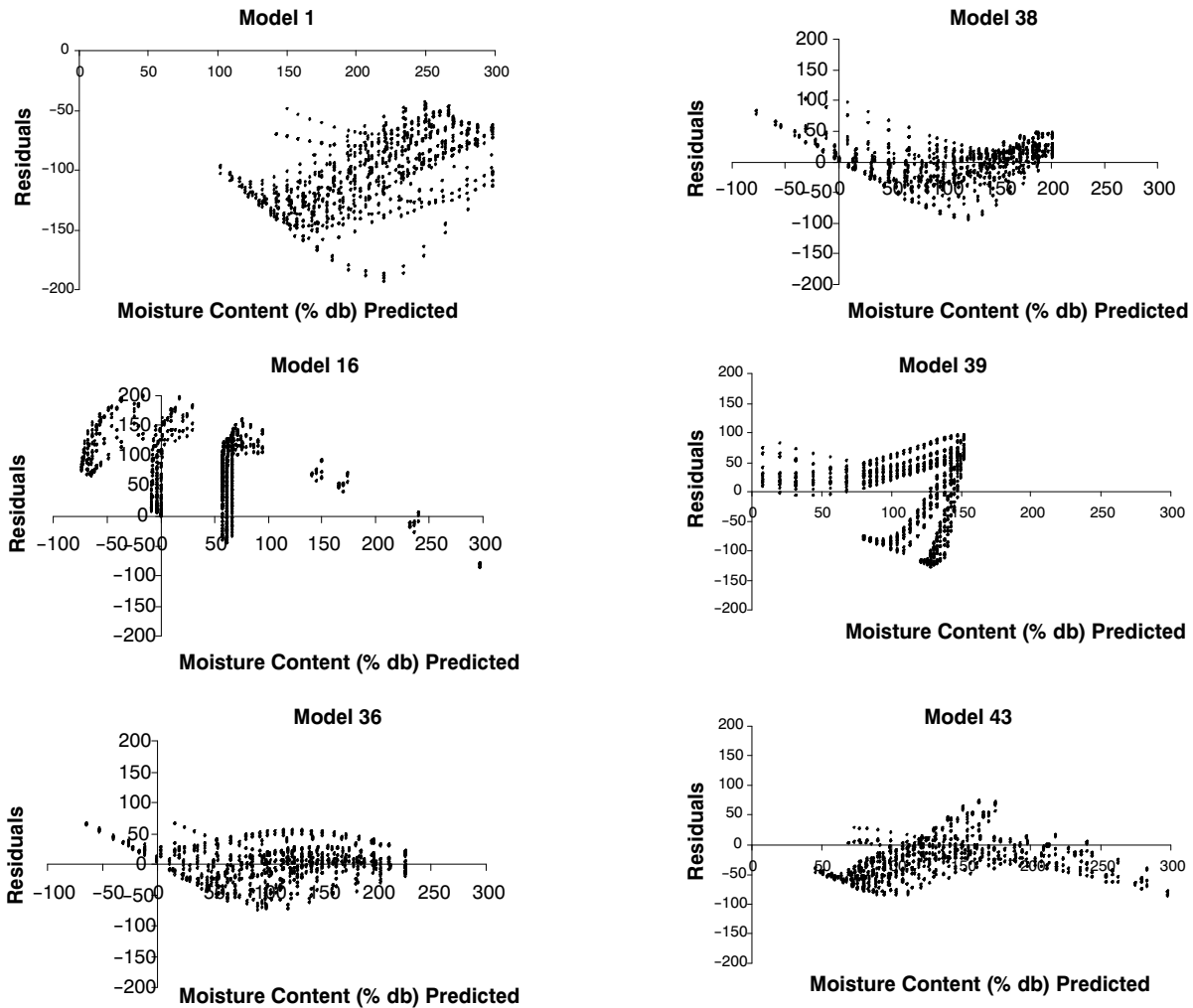
Figure 2. Residual plots for selected moisture content (% db) vs. time models from table 1. All residual plots indicated the inadequacy of the moisture content modeling efforts, as shown by shifts and patterns observed in the residuals.

moisture ratio over time. Similar to our findings for the desorption behavior of DWG, the Page model was found to work well for the thin layer drying of apricots and wheat grains (Menges and Ertekin, 2006; Goneli et al., 2007). Doymaz (2005) also found that Page's model was a better statistical fit than either the Lewis model or the Henderson and Pabis model (Henderson and Pabis, 1961), for moisture ratio versus time modeling of green beans.

The definition we used for MR is appropriate when there is constant level of relative humidity in the drying air (e.g. laboratory drying conditions) (Midilli et al., 2002).

Figure 3a presents a plot of predicted moisture ratio (MR) values (superimposed with the actual data) using the basic Page model (eq. 2, table 3), while figure 3b presents plots of moisture ratio versus time using the optimal model for our data (model G4, table 4), which also includes temperature and CDS terms. From figure 3b, we can clearly observe that there was a strong relationship between drying temperature and moisture ratio; three distinct predicted moisture ratio lines for 100°C, 200°C, and 300°C were prominently observed. It was also evident that the time taken to reduce the moisture content was longer for 100°C compared to 200°C, which in turn was greater than that for 300°C. This was anticipated *a priori*. However, the drying time for each

respective temperature level changed little amongst CDS levels.

From figure 3b at 100°C for the 10% CDS level, we can see that there was some over-prediction for times greater than 35 min, while there were some under predictions for the 20% CDS levels. This was probably due to scatter in the experimental data (i.e., experimental error). Similar patterns were also found in figure 3a where the basic Page model was used. Our model fitting graphs were similar to many other drying studies (Ozdemir and Devres, 1999; Sogi et al., 2003; Menges and Ertekin, 2006; Doymaz, 2005; Kingsly and Singh, 2007).

From figure 4 we can see the nature of residuals for various models. For example, using the Newton model (table 3, eq. 1) for each drying temperature and CDS level, patterns were observed in the residuals, which was not desirable (Draper and Smith, 1998). Figure 4 also indicates the residual plot for the global equation using our selected optimum model (eq. G4, table 4) where CDS and temperature parameters were incorporated. This was an overall comprehensive model for moisture ratio versus time for DWG. There were no negative predicted MR values observed in the residual plots; however, in some cases, we could observe curved patterns in the residual plots, which suggests that higher order terms may be necessary for these model equations. Such
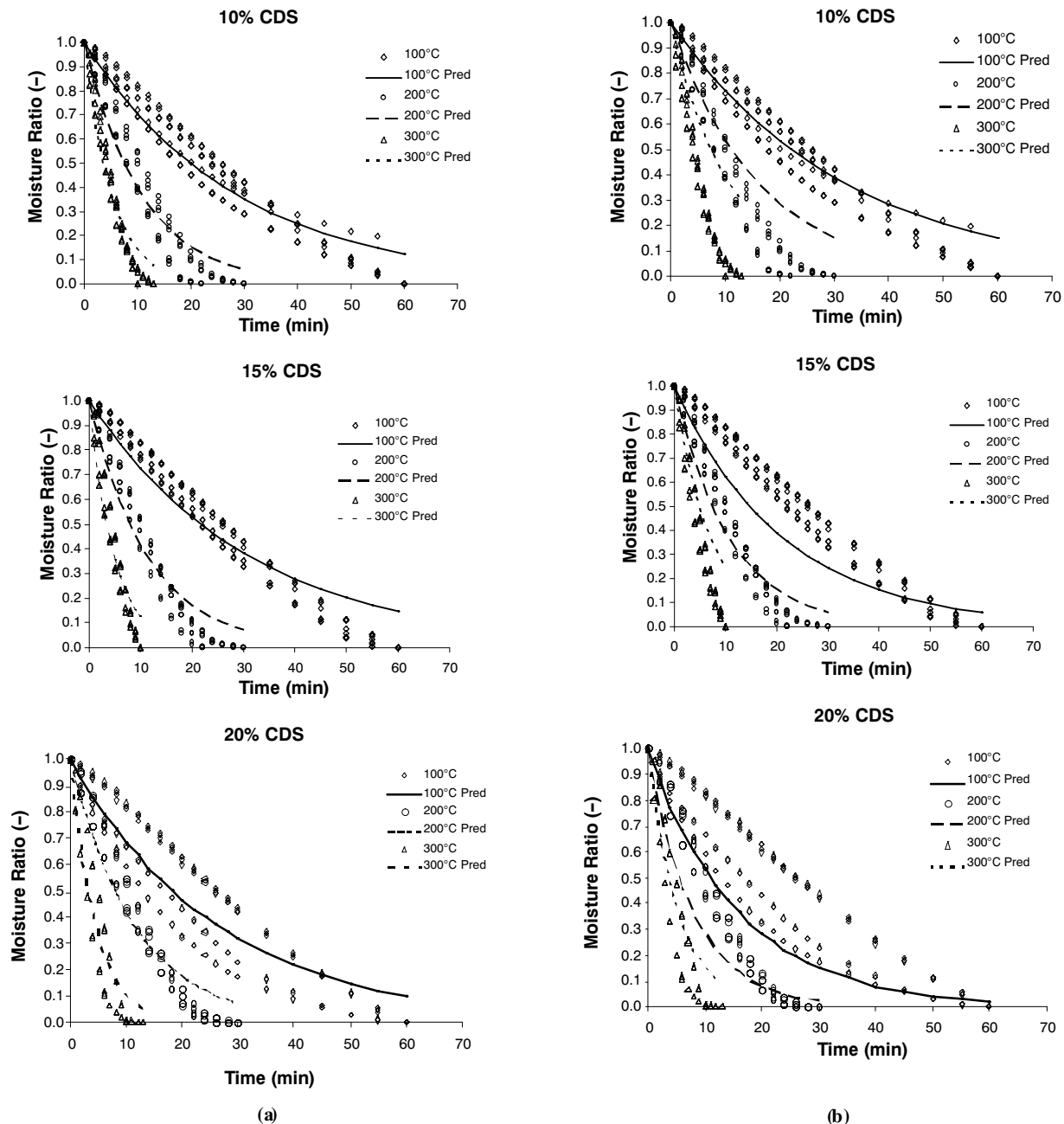
Figure 3. (a) Plot of moisture ratio vs. time using the basic Page Model (eq. 2, table 3) for each CDS/temperature level combination (i.e., the model was applied to each combination individually). (b) Plot of moisture ratio vs. time using Modified Page Model 1 (eq. G4, table 4), which was the best overall comprehensive global equation that modeled all collected data, for all CDS/temperature combinations simultaneously.

shortcomings were alleviated in the global model (eq. G4, table 4), which resulted in a random distribution of residuals, as shown in figure 4. This strongly suggests that our goal of developing a global model was successful.

The usefulness of this research arises from the ability to predict required drying times which are necessary at a given temperature and CDS addition level in order to achieve a specified final moisture content in the DDGS. Our final equation will, of course, need to be verified and validated on commercial-scale drying equipment at a fuel ethanol plant. But this study has served as a good starting point, as no one else has examined or published this kind of drying analysis to date.

CONCLUSIONS

The drying behavior of DWG to produce DDGS, using three CDS addition levels (10%, 15%, and 20% wb) and three drying temperature levels (100°C, 200°C, and 300°C) was determined. Comprehensive models for moisture ratio versus time (based on the Page model) which also included terms for CDS addition and drying temperature levels were found effective in predicting moisture ratios (eq. G4, table 4) for DWG desorption. This first step towards understanding drying of DDGS will be useful in predicting drying behavior under varying operating conditions which are often seen in industry. It can also be used to predict the total drying time required to achieve a desired moisture content for various
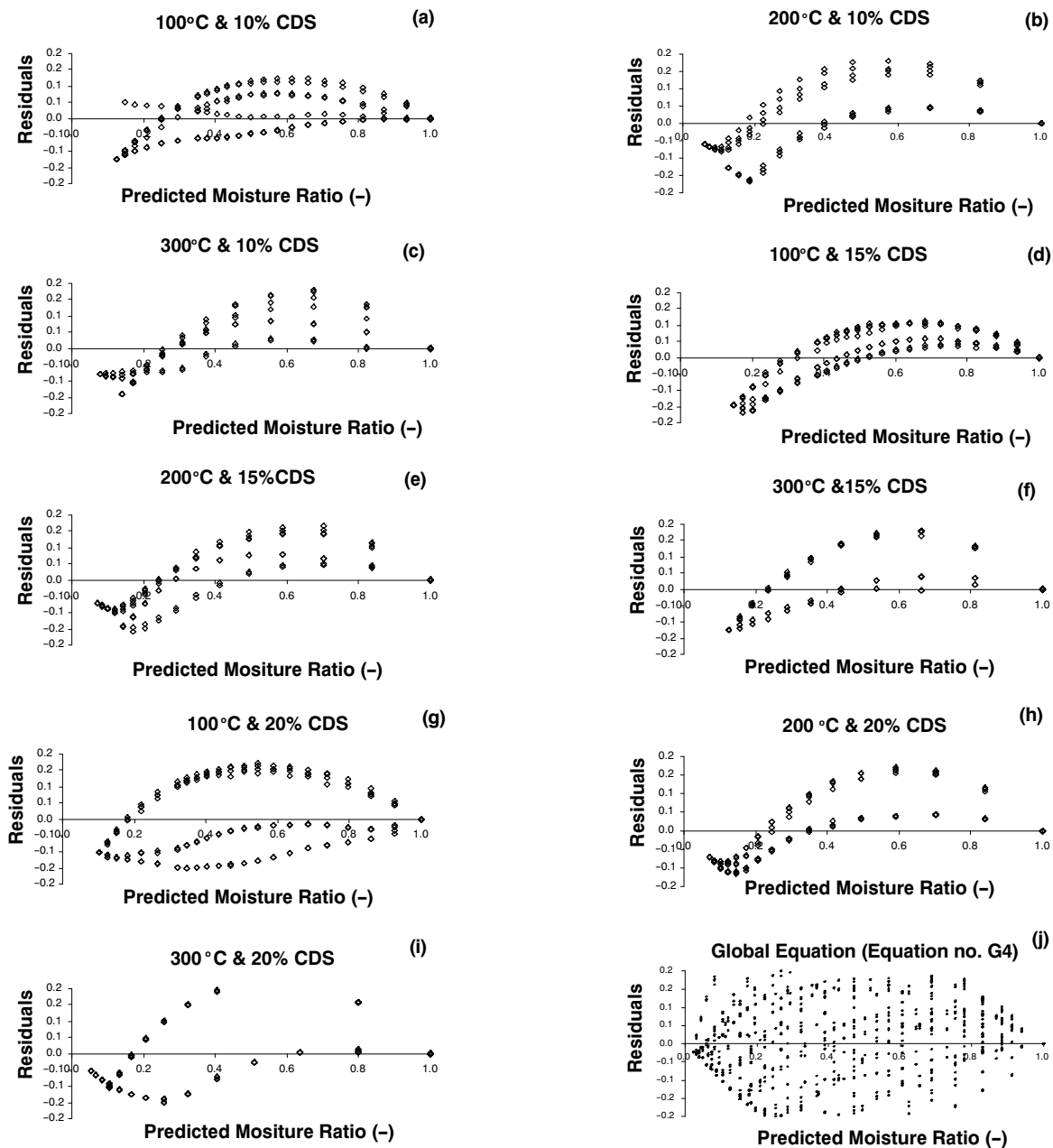
Figure 4. Residual plots for selected Moisture Ratio (–) models. (a) through (i) Newton model (table 2, eq. 1) results (a) k=0.0348; (b) k=0.0933; (c) k=0.1964; (d) k=0.032; (e) k=0.0885; f) k=0.2073; (g) k=0.03799; (h) k=0.088; (i) k=0.2258; (j) Global equation (based on modified Page model, eq. G4, table 3), k=0.00148, n=0.02 – note that the residuals are randomly scattered for this model.

practical settings. Since there have been no developed models or drying simulation studies for DDGS to date, this research will be a step towards such research areas. Future studies with higher CDS levels and other drying temperatures should also be evaluated.

REFERENCES

AAFC Bulletin. 2006. Protein meal: Situation and outlook. *Agriculture and Agri-Food Canada, Bi-Weekly Bulletin* 19(3): 1-4.

Ayensu, A. 1997. Dehydration of food crops using solar dryer with convective heat flow. *Solar Energy* 59(4): 121-126.

Barta, P. 2008. As biofuels catch on, next task is to deal with environmental, economic impact. *Wall Street Journal* March 24: pg. A2.

Bhadra, R., K. Muthukumarappan, and K. A. Rosentrater. 2009a. Flowability properties of commercial distillers dried grains with solubles. *Cereal Chemistry* 86(2): 170-180.

Bhadra, R., K. A. Rosentrater, and K. Muthukumarappan. 2009b. Cross-sectional staining and surface properties of DDGS particles and their influence on flowability. *Cereal Chemistry* 86(4): 410-420.

Bharatan, M., D. J. Schingoethe, A. R. Hippen, K. F Kalscheur, M. L. Gibson, and K. Karges. 2008. Conjugated linoleic acid increases in milk from cows fed condensed corn distillers solubles and fish oil. *J. Dairy Science* 91(7): 2796-2807.

Carr, R. L., Jr. 1965. Evaluating flow properties of solids. *Chemical Eng.* 72(3): 163-168.

Cheesbrough, V., K. A. Rosentrater, and J. Visser. 2008. Properties of distillers grains composites: A preliminary investigation. *J. Polymers and the Environment* 16(1): 40-50.

Domyaz, I. 2005. Drying behavior of green beans. *J. Food Eng.* 69(2): 161-165.

Draper, N. R., and H. Smith. 1998. *Applied Regression Analysis.* New York, N.Y.: John Wiley and Sons, Inc.

Ganesan, V., K. A. Rosentrater, and K. Muthukumarappan. 2007a. Physical and flow properties of regular and reduced fat distillers dried grains with solubles (DDGS). *Food and Bioprocess Tech.* 2(2): 156-166.

Ganesan, V., K. A. Rosentrater, and K. Muthukumarappan. 2007b. Dynamic water adsorption characteristics of distillers dried grains with solubles. *Cereal Chemistry* 84(6): 584-555.

Ganesan, V., K. A. Rosentrater, and K. Muthukumarappan. 2007c. Modeling the flow properties of distillers dried grains with solubles (DDGS). *Cereal Chemistry* 84(6): 556-562.

Ganesan, V., K. Muthukumarappan, and K. Rosentrater. 2008a. Effect of flow agent addition on physical properties of DDG with varying moisture content and soluble percentages. *Trans. ASABE* 51(2): 591-601.

Ganesan V., K. Muthukumarappan, and K. A. Rosentrater. 2008b. Sorption isotherm characteristics of distillers dried grain with solubles (DDGS). *Trans. ASABE* 51(1): 169-176.

Ganesan, V., K. Muthukumarappan, and K. A. Rosentrater. 2008c. Effect of moisture content and soluble level on the physical, chemical, and flow properties of distillers dried grains with solubles (DDGS). *Cereal Chemistry* 85(4): 464-470.

Ganesan, V., K. A. Rosentrater, and K. Muthukumarappan. 2008d. Flow properties of DDGS with varying soluble and moisture contents using Jenike shear testing. *J. Powder Tech.* 187: 130-137.

Goneli, A. L. D., P. C. Correa, and M. A. Martins. 2007. Mathematical modeling of thin-layer drying kinetics of wheat. ASABE Paper No: 076193. St Joseph, Mich.: ASABE.

Greenquist, M., T. J. Klopfenstein, W. H. Schact, and G. E. Erickson. 2009. Replacing fertilizer nitrogen with distillers grains supplements to yearling steers grazing Bromegrass pastures: economics and modeling. Nebraska Beef Cattle reports. University of Nebraska-Lincoln. Available at: digitalcommons.unl.edu/animalscinbcr/500. Accessed 8 March 2010.

Henderson, S. M., and S. Pabis. 1961. Grain drying theory: I. Temperature effect on drying coefficients. *J. Agric. Eng. Res.* 6(3): 169-174.

Jenike, A. W. 1964. Storage and flow of solids. Bulletin No. 123. Utah Engineering Station. Salt Lake City, Utah: University of Utah.

Kingsly, A. R. P., and D. B. Singh. 2007. Drying kinetics of pomegranate arils. *J. Food Eng.* 79(2): 741-744.

Kleinschmit, D. H., D. J. Schingoethe, K. F. Kalscheur, and A. R. Hippen. 2006. Evaluation of various sources of corn distillers grains plus solubles for lactating dairy cattle. *J. Dairy Sci.* 89(12): 4784-4794.

Kleinschmit, D. H., D. J. Schingoethe, K. F. Kalscheur, and A. R. Hippen. 2007. Dried distillers grains plus solubles with corn stillage or alfalfa hay as the primary forage source in dairy cow diets. *J. Dairy Sci.* 90(12): 5587-5599.

Mendoza, M. G. V., C. M. Vera, and F. V. C Dominguez. 2003. Thermal and moisture diffusion properties of amaranth seeds. *Biosystems Eng.* 86(4): 441-446.

Menges, H. O., and C. Ertekin. 2006. Modelling of air drying of hacihaliloglu-type apricots. *J. Science of Food and Agric.* 86(2): 279-291.

Midilli, A., H. Kucuk, and Z. Yapar. 2002. A new model for single layer drying. *Drying Tech.* 20(7): 1503-1513.

Mjoun, K., K. F Kalscheur, D. J. Schingoethe, and A. R. Hippen. 2007. In situ ruminal phosphorus availability from corn and soybean feedstuffs. *J. Dairy Sci.* 90(10): 3939-3946.

Mpapho, G. S., A. R. Hippen, K. F. Kalscheur, and D. J. Schingoethe. 2007. Production responses of dairy cows fed wet distillers grains during the transition period and early lactation. *J. Dairy Sci.* 90(Suppl. 1): (abstr.) 3080.

Ozdemir, M., and Y. O. Devres. 1999. The thin layer drying characteristics of hazelnuts during roasting. *J. Food Eng.* 42(4): 225-233.

Pabis, S., D. S. Jayas, and S. Cenkowski. 1998. *Grain Drying.* New York, N.Y.: John Wiley and Sons, Inc.

Peleg, M. 1988. An empirical model for description of moisture sorption curves. *J. Food Sci.* 53(4): 1216-1219.

Pilosof, A. M. R., R. Boquet, and G. B. Bartholomai. 1985. Kinetics of water uptake by food powders. *J. Food Sci.* 50(2): 278-282.

Renewable Fuels Association (RFA). 2010 Industry Resources Coproducts. Available at: www.ethanolrfa.org/industry/reseources/coproducts/ Accessed 8 March 2010.

Rock, M., and J. Schwedes. 2005. Investigations on the caking behavior of bulk solids - macroscale experiments. *Powder Tech.* 157(1-3): 121-127.

Rosentrater, K. A., and K. Muthukumarappan. 2006. Corn ethanol coproducts: Generation, properties, and future prospects. *Intl. Sugar J.* 108(1295): 648-657.

SAS. 2002. *SAS User's Guide: Statistics*. Ver. 6a. Cary, N.C.: SAS Institute, Inc.

Seber, G. A., and C. J. Wild. 1989. *Nonlinear Regression.* New York, N.Y.: John Wiley and Sons, Inc.

Sharaf-Elden, O., Y. I. Blaisdell, and G. Spagna. 1980. A model for ear corn drying. *Trans. ASAE* 23(5): 1261-1271.

Sharma, G. P., S. Prasad, and A. K. Datta. 2003. Drying kinetics of garlic cloves under convective drying conditions. *J. Food Sci. and Tech.* 37(5): 520-522.

Simal, S., A. Femenia, M. C. Garau, and C. Rosselló. 2005. Use of exponential, Page's and diffusional models to simulate the drying kinetics of kiwi fruits. *J. Food Eng.* 66(3): 323-328.

Singh, B. P. N., and S. P. Kulshrestha. 1987. Kinetics of water sorption by soybean and pigeon pea grains. *J. Food Sci.* 52(5): 1538-1541, 1544.

Sogi, D. S., U. S Shivhare, S. K. Garg, and A. S. Bawa. 2003. Water sorption isotherm and drying characteristics of tomato seeds. *Biosystems Eng.* 84(3): 297-301.

Speihs, M. J., M. H. Whitney, and G. C. Shurson. 2002. Nutrient database for distillers dried grains with solubles produced from new ethanol plants in Minnesota and South Dakota. *J. Animal Sci.* 80(10): 2639-2645.

Tan, D. L. S., K. Miyamoto, K. Ishibashi, K. Matsuda, and T. Satow. 2001. Thin layer drying of sweet potato chips and pressed grates. *Trans. ASAE* 44(3): 669-674.